Biochimica et Biophysica Acta 1783 (2008) 2301–2310

Contents lists available at ScienceDirect

Biochimica et Biophysica Acta

journal homepage: www.elsevier.com/locate/bbamcr

Accessory subunit Ac45 controls the V-ATPase in the regulated secretory pathway

Eric J.R. Jansen [a], Wim J.J.M. Scheenen [b], Theo G.M. Hafmans [a], Gerard J.M. Martens [a,*]

[a] Department of Molecular Animal Physiology, Donders Centre for Neuroscience and Nijmegen Centre for Molecular Life Sciences (NCMLS), Faculty of Science, Radboud University, Geert Grooteplein Zuid 28, 6525 GA Nijmegen, The Netherlands
[b] Department of Cellular Animal Physiology, Donders Centre for Neuroscience and European Graduate School for Neurosciences (EURON), Faculty of Science, Radboud University, Heyendaalseweg 135, 6525 AJ Nijmegen, The Netherlands

ARTICLE INFO

Article history:
Received 20 March 2008
Received in revised form 26 June 2008
Accepted 26 June 2008
Available online 8 July 2008

Keywords:
Xenopus transgenesis
Ca^{2+}-dependent peptide secretion
Intermediate pituitary melanotrope cells
Proton pump trafficking
Secretory capacity
Plasma membrane protrusions

ABSTRACT

The vacuolar (H^+)-ATPase (V-ATPase) is crucial for multiple processes within the eukaryotic cell, including membrane transport and neurotransmitter secretion. How the V-ATPase is regulated, e.g. by an accessory subunit, remains elusive. Here we explored the role of the neuroendocrine V-ATPase accessory subunit Ac45 via its transgenic expression specifically in the *Xenopus* intermediate pituitary melanotrope cell model. The Ac45-transgene product did not affect the levels of the prohormone proopiomelanocortin nor of V-ATPase subunits, but rather caused an accumulation of the V-ATPase at the plasma membrane. Furthermore, a higher abundance of secretory granules, protrusions of the plasma membrane and an increased Ca^{2+}-dependent secretion efficiency were observed in the Ac45-transgenic cells. We conclude that in neuroendocrine cells Ac45 guides the V-ATPase through the secretory pathway, thereby regulating the V-ATPase-mediated process of Ca^{2+}-dependent peptide secretion.

1. Introduction

The vacuolar (H^+)-ATPase (V-ATPase) is a multi-subunit enzyme complex that resides in the plasma membrane and in membranes of various subcellular compartments, such as endosomes, lysosomes and secretory vesicles. The V-ATPase is of crucial importance for a variety of cell-biological events that depend on active proton transport across a membrane to establish organelle acidification or to generate a transmembrane electrical potential, thereby affecting processes such as embryonic left–right patterning, osteoclastic bone resorption, intracellular membrane transport, endosomal receptor–ligand dissociation, lysosomal hydrolysis, receptor-mediated endocytosis, intracellular protein targeting, prohormone sorting and processing, and neurotransmitter uptake [1–4]. Intriguingly, recent data suggest a role for the V-ATPase in membrane fusion during exocytotic secretion as well [5–8].

V-ATPases are present in virtually all eukaryotic cells, but their molecular composition and subcellular localizations differ between organisms and cell types (reviewed in [9]). The enzyme consists of two domains, the peripheral V_1-domain responsible for ATP hydrolysis and the integral V_0-domain which takes care of the proton transport over the membrane [3]. At present, surprisingly little is known about the targeting and regulation of the V-ATPase. Although V_1–V_0 association/dissociation is thought to be a universal mechanism for regulating V-ATPase activity [9], other regulatory mechanisms have been proposed, such as an interaction of the V-ATPase complex with an accessory subunit [10,11]. The type I transmembrane glycoprotein Ac45 is such a V-ATPase accessory subunit. The neuronal- and neuroendocrine-enriched Ac45 protein was first isolated from bovine chromaffin granules by its co-purification with the V_0-sector of the pump ([10,12], reviewed in [13]). Subsequently, analysis of the V_0-complex [14] and a recent co-immunoprecipitation study in transfected COS-7 cells [4] confirmed the association of Ac45 with the V_0-subunits of the membrane sector.

In *Xenopus laevis* intermediate pituitary melanotrope cells, Ac45 has been found to be coordinately expressed with the prohormone proopiomelanocortin (POMC) [15]. In the early secretory pathway of these cells, the Ac45 protein is proteolytically processed to a C-terminal cleavage product that corresponds to the mammalian Ac45 protein isolated from secretory granules [16,17]. The neuroendocrine *Xenopus* melanotrope cells can be activated in vivo to produce large amounts of POMC simply by placing the animal on a black background. POMC is cleaved by prohomone convertases (PCs) to a number of bioactive peptides, including α-melanophore stimulating hormone (α-MSH) that is released into the bloodstream, causing dispersion of the skin melanophores [18]. In contrast to cultured neuroendocrine cell lines, the *Xenopus* melanotropes are strictly regulated cells with the prohormone and other regulated secretory proteins sorted efficiently into secretory granules [19]. Peptide release from the melanotrope cells occurs exclusively via the regulated secretory pathway with the second messenger Ca^{2+}as the driving force for α-MSH release [20–22].

Although Ac45 has been identified more than a decade ago, its role is still elusive. In view of its coordinated expression with POMC, we

* Corresponding author. Tel.: +31 24 3610564; fax: +31 24 3615317.
E-mail address: g.martens@ncmls.ru.nl (G.J.M. Martens).

0167-4889/$ – see front matter © 2008 Elsevier B.V. All rights reserved.
doi:10.1016/j.bbamcr.2008.06.020

have proposed a role for Ac45 in the regulated secretory pathway [15,16]. In a first attempt to study its function, we previously disrupted the Ac45 gene in the mouse but unfortunately blastocyst development was severely affected, resulting in early embryonic lethality [23]. To explore the function of Ac45 in an in vivo context and in a well-defined model system, we now combined the unique features of the *Xenopus* melanotrope cell with the technique of stable *Xenopus* transgenesis [24,25]. We used a *Xenopus* POMC-gene promoter fragment [26] to target transgene expression of intact Ac45 or cleaved Ac45 specifically to the melanotrope cells. This cell-specific transgenic approach enabled us to examine the melanotrope cells with the regulatory input from the hypothalamic neurons being unaffected. Here we describe the effects of excess Ac45 on the functioning of the regulated secretory pathway in the melanotrope cells. The results of our study are most consistent with a role for Ac45 in V-ATPase routing and in this way controlling the V-ATPase in the regulated secretory pathway.

2. Material and methods

2.1. Animals

Xenopus laevis were reared in the *Xenopus* facility of the Department of Molecular Animal Physiology (Central Animal Facility, Radboud University Nijmegen). Experimental animals were adapted to a black background for 3 up to 8 weeks with a light/dark cycle of 12 h. All animal experiments were carried out in accordance with the European Communities Council Directive 86/609/EEC for animal welfare, and permits GGO 98-143 and RBD0166(H10) to generate and house transgenic *Xenopus laevis*.

2.2. Generation of Xenopus laevis stably transgenic for intact-Ac45 or cleaved-Ac45 fused to GFP

Since the C-tail of the *Xenopus* Ac45 protein contains putative targeting signals [27] and to avoid any possible trafficking defect, GFP was fused to the N-terminus of Ac45. To translocate the fusion proteins over the ER membrane, the *Xenopus* Ac45 signal peptide (SP) sequence was placed in front of GFP. To generate DNA encoding intact-Ac45 or cleaved-Ac45, the *Xenopus* Ac45 ORF (clone X1311-4 [16], lacking the signal peptide) was amplified by PCR (High Fidelity PCR Mix; MBI Fermentas), using forward primer 5′-gggggaattccag-caagtgcccgtgctg-3′ and reverse primer 5′-ggggtctagattactctgtctgggg-cacagc-3′, or forward primer 5′-gggggaattccctatgccaagctatcctcc-3′ and reverse primer 5′-ggggtctagattactctgtctggggcacagc-3′, respectively. The EcoRI/XbaI-digested intact-Ac45 or cleaved-Ac45 PCR products were subcloned into the pPOMC(A)$^{2+}$-SP-GFP vector [28] resulting in the constructs pPOMC(A)$^{2+}$-GFP/intact-Ac45 and pPOMC (A)$^{2+}$-GFP/cleaved-Ac45, respectively. To generate transgenic *Xenopus laevis*, 125 ng of purified SalI/NotI linear DNA fragments from pPOMC (A)$^{2+}$-GFP/intact-Ac45 and pPOMC(A)$^{2+}$-GFP/cleaved-Ac45 containing the SV40-polyA signal were used for stable *Xenopus* transgenesis [26]. Several transgenesis rounds yielded transgenic F0 *Xenopus* embryos with various transgene expression levels in the pituitary as was judged by direct screening of the living embryos under a fluorescence microscope (Leica MZ FLIII). To generate F1 offspring, testes of transgenic F0 *Xenopus* males were used to fertilize in vitro wild-type *Xenopus* eggs resulting in transgenic lines #452 and #465 expressing GFP/intact-Ac45, and lines #533 and #604 expressing GFP/cleaved-Ac45 specifically in the intermediate pituitary melanotrope cells.

2.3. Antibodies

The rabbit polyclonal antibody raised against the C-terminal region of *Xenopus* Ac45 (1311-C) has been described previously [16]. A rabbit polyclonal antibody raised against GFP was kindly provided by Dr. B. Wieringa [29], and against POMC (ST62) [30], V-ATPase subunit V_1A (ST170) and subunit V_1E (ST173) [31] by Dr. S. Tanaka (Shizuoka University, Japan). Monoclonal anti-tubulin antibody E7 has been described previously [32]. The rabbit antiserum against *Xenopus* V-ATPase subunit V_0a (ST205) was raised against a synthetic peptide comprising 14 amino acid residues located in the cytoplasmic domain of *Xenopus* V_0a with an additional cysteine at the N-terminus (CMQTNQTPPTYNKTN). The rabbit antiserum against *Xenopus* V_0d (ST200) was raised against a synthetic peptide comprising 13 amino acid residues located in the N-terminal part of *Xenopus* V-ATPase subunit V_0d with an additional cysteine at the N-terminus (CVSVIDDKLKEKMV).

2.4. Cryosectioning and immunohistochemistry

Brain-pituitary preparations were dissected from juvenile transgenic frogs and fixed in 4% paraformaldehyde in PBS. After cryoprotection in 10% sucrose-PBS, sagittal 20 μm cryosections were mounted on poly-L-lysine-coated slides and dried for 2 h at 45 °C.

For immunohistochemistry, sections were rinsed for 30 min in 50 μM Tris-buffered saline (pH 7.6) containing 150 μM NaCl and 0.1% Triton X-100 (TBS-TX). To prevent nonspecific binding, blocking was performed with 0.5% BSA in TBS-TX. Sections were incubated with anti-POMC (ST62, 1: 2000) or anti-V-ATPase subunit V_1A (ST170, 1:500) antibodies for 16 h at 37 °C in TBS-TX containing 0.5% BSA. After rinsing the slides with TBS-TX, a second antibody, Goat-anti-Rabbit-Alexa Fluor 568 (Molecular Probes, Eugene, Oregon, USA) at a dilution of 1:100, was applied and sections were incubated for 1 h at 37 °C. Following an additional washing step, the sections were mounted in Mowiol (Sigma) containing 2.5% sodium azide and coverslipped. Immunofluorescence was viewed under a Leica DMRA fluorescence microscope and a Biorad MRC 1024 confocal laser scanning microscope.

2.5. Isolation of Xenopus intermediate pituitary melanotrope cells and Western blot analysis

Since the neural lobe contains substantial amounts of the Ac45 protein, we performed Western blot analysis on lysates of melanotrope cells isolated from neurointermediate lobes (NILs) to study the endogenous Ac45 protein level. The melanotrope cells were isolated from *Xenopus* NILs essentially as described previously [16], washed with XL15 medium, collected by centrifugation and lysed in lysis buffer (50 mM HEPES pH 7.4, 140 mM NaCl, 0.1% Triton X-100, 1% Tween 20, 2% CHAPS, 1 mg/ml deoxycholate, 1 μM phenylmethylsulfonyl fluoride (PMSF), 0.1 mg/ml soy bean trypsin inhibitor). Total protein content of the cell lysates was measured using the Micro BCA™ Protein Assay kit (Pierce, Rockford) according to the manufacturer's prescription. 10 μg of protein lysate was incubated in the presence or absence of *N*-glycosidase F (Roche Diagnostics, Mannheim) before loading on 10% SDS-PAGE. Western blots were incubated with an anti-Ac45 antibody (anti-X1311-C, 1:5000), an anti-GFP antibody (1:5000), anti-V-ATPase subunit V_1A, V_1E, V_0a and V_0d antibodies (1:2000, ST170, ST173, ST205 and ST205, respectively), anti-POMC (1:10000, ST62) or anti-tubulin (1:100, monoclonal antibody E7) and secondary peroxidase-conjugated Goat-anti-rabbit antibody followed by chemoluminescence. Signals were detected and quantified using a BioImaging system with Labworks 4.0 software (UVP BioImaging systems, Cambridge, UK). For confocal laser scanning microscopy (CLSM) and patch-clamp experiments, the isolated melanotrope cells were cultured on cover slips.

2.6. Metabolic cell labeling and immunoprecipitations

For radioactive labeling of newly synthesized proteins, freshly isolated *Xenopus* NILs were pre-incubated for 10 min in Ringer's

medium containing 0.3 mg/ml BSA (Ringer's/BSA), then incubated in Ringer's/BSA containing 1.7 mCi/ml Tran^{35}S label (MP Biomedicals) for indicated time periods and subsequently chased in Ringer's/BSA or *Xenopus* L15 medium supplemented with 0.5 mM L-methionine. Lobes were lysed in 100 µl lysis buffer without CHAPS, and lysates were cleared by centrifugation (13,000 *g*, 7 min) and directly analysed by SDS-PAGE. For immunoprecipitations, lysates were supplemented with 0.08% SDS and incubated with the anti-GFP (1:500) or the anti-Ac45 (anti-X1311-C, 1:500). Immune complexes were precipitated with protein-A Sepharose (Amersham Pharmacia Biotech), analyzed by SDS-PAGE and visualized by fluorography.

2.7. Cm measurements

Membrane capacitance (Cm) measurements were performed in the whole-cell configuration of the patch-clamp technique using a computer-based patch-clamp amplifier (EPC-9) controlled by Pulse software, V. 8.63 (HEKA, Lambrecht/Pfalz, Germany) [33]. Data were filtered by a Bessel filter set at 12.9 kHz. Patch pipettes were pulled from Wiretrol II glass capillaries (Drummond Scientific, Broomall, PA, USA) using a PP-83 pipette puller (Narishige Scientific Instrument Laboratories, Tokyo, Japan), and had a resistance between 3 and 5 MΩ after polishing. The external solution contained 93 mM TEACl, 5 mM CsCl, 2 mM $MgCl_2$, 2 mM $CaCl_2$, 10 mM glucose and 15 mM HEPES, adjusted to pH 7.4 with TEAOH. The internal solution contained 112 mM CsCl, 1.8 mM $MgCl_2$, 2 mM MgATP, 0.1 mM EGTA and 10 mM HEPES, adjusted to pH 7.2 with CsOH. The sampling rate of Ca^{2+}-currents was 2500 Hz. Cm was measured in the 'sine+dc' mode of the lock-in extension of the Pulse software, based on the Lindau–Neher algorithm [34] using an 800-Hz, 40-mV peak-to-peak sinusoid stimulus. After the whole-cell configuration was established, Cm was recorded and cancelled by the automatic capacitance compensation of the EPC-9. The procedure was repeated every 60 s (Cslow-update of the EPC-9 amplifier) to prevent saturation of the lock-in signal [34]. In order to avoid any possible artifacts in the Cm trace induced by the membrane conductance, the first 50 ms of the Cm trace were not taken into account.

2.8. (Immuno)Electron microscopy

Xenopus NILs were freshly dissected, fixed, osmicated, dehydrated and embedded in Epon 812. Ultra-thin sections were cut, double-contrasted with uranyl acetate/lead citrate and photographed using a transmission microscope (JEOL1010). For freeze substitution and low-temperature embedding, the tissue was rapidly frozen by a Leica electron microscopy (EM) High-Pressure Freezing system (Leica Microsystems) followed by freeze substitution. The tissue was then immersed in acetone containing 0.5% uranyl acetate as fixing agent at −90 °C. The temperature was raised stepwise to −45 °C and the tissue was then infiltrated with Lowicryl HM20. Thin sections were cut and mounted on one-hole nickel grids coated with a formvar film.

For postembedding immunohistochemistry, ultra-thin Lowicryl sections were washed for 10 min in phosphate buffered saline (PBS, pH 7.4) containing 0.1% sodium borohydride and 50 mM glycine, and for 10 min in PBS containing 0.5% BSA and 0.1% cold fish skin gelatine (PBG). For immunolabeling, sections were incubated overnight at 4 °C in drops of PBG containing anti-GFP (1:500), anti-POMC (ST62; 1:15000) or anti-V-ATPase subunit V_1A, V_1E, V_0a and V_0d antibodies (ST170, ST173, ST205 and ST200, respectively; 1:50). Sections were washed for 20 min in PBG, incubated with protein-A-labeled 10 nm gold markers, washed in PBS and postfixed with 2.5% glutaraldehyde in PB for 5 min to minimize loss of gold label during the contrasting steps. After washing with distilled water, sections were contrasted in uranyl acetate and studied using a Jeol transmission electron microscopy (TEM) 1010 electron microscope.

2.9. Statistics

Data are presented as means±SEM. Statistical evaluation was performed using an unpaired Student's *t*-test.

3. Results

3.1. Generation of stable transgenic Xenopus laevis expressing a GFP/intact-Ac45 or GFP/cleaved-Ac45 fusion protein specifically in the intermediate pituitary melanotrope cells

In vivo, intact *Xenopus* Ac45 (~62 kDa) is proteolytically processed to an ~40 kDa cleaved C-terminal fragment [16,17]; the mammalian ~45-kDa Ac45 protein that was originally isolated from secretory granules corresponds to the cleaved C-terminal fragment [10]. To study the function of Ac45, we generated stable transgenic *Xenopus laevis* lines expressing intact or cleaved *Xenopus* Ac45 fused to the green fluorescent protein GFP. A *Xenopus* POMC-gene promoter fragment [26] was used to drive transgene expression specifically to the intermediate pituitary melanotrope cells (Fig. 1A). Fluorescence was exclusively detected in the intermediate pituitary from developmental stage-40 onwards and no difference was observed between transgenic and wild-type tadpoles regarding the development of the pituitaries. Embryos were further cultured and stage-45 living embryos could be readily screened for fluorescent protein expression in the pituitary by direct visual inspection under a fluorescence microscope (Fig. 1B). In vitro fertilization with sperm derived from testes of transgenic *Xenopus* males resulted in two independent stable transgenic *Xenopus* F1 lines expressing GFP/intact-Ac45 (lines #452 and #465) and two independent stable transgenic F1 lines expressing GFP/cleaved-Ac45 (lines #533 and #604).

Direct fluorescence microscopy on cryosections of pituitaries of adult transgenic F1 animals clearly showed that the transgene expression was exclusively in the intermediate pituitary melanotrope cells, shown by co-localization with the main melanotrope secretory cargo protein POMC (Fig. 1C). CLSM and EM revealed that in both #452- and #465-transgenic melanotrope cells the GFP/intact-Ac45 transgene product was localized mainly to the ER, indicating that the protein was not efficiently transported through the secretory pathway. In contrast, in both #533- and #604-transgenic cells the GFP/cleaved-Ac45 transgene product was localized primarily to the plasma membrane of the melanotrope cells (Fig. 1D). Immuno-EM using an anti-GFP antibody confirmed the absence of GFP/intact-Ac45 and the presence of GFP/cleaved-Ac45 at the plasma membrane (Fig. 1E). Lines #452 and #533 were selected for the further analysis of melanotrope cells expressing GFP/intact-Ac45- and GFP/cleaved-Ac45, respectively.

To study the steady-state transgenic protein expression levels, we isolated both the neurointermediate lobe (NIL) and the anterior lobe (AL) of the pituitary. Western blot analysis of the NIL lysates from wild-type animals using an anti-Ac45-C antibody showed an ~40-kDa product representing the endogenous Ac45 protein (Fig. 2A). In the GFP/intact-Ac45 transgenic NIL lysates, an ~90-kDa protein corresponding to the GFP/intact-Ac45 transgene fusion product was detected by both an anti-GFP and the anti-Ac45-C antibody. Only a minor portion of this product was cleaved to an ~50-kDa protein representing the N-terminal part of GFP/intact-Ac45. The GFP/cleaved-Ac45 transgene product was found as an ~70-kDa product. No transgene products were found in the lysates of the AL, illustrating the melanotrope cell specificity of the POMC-gene promoter fragment (Fig. 2A).

To study the biosynthesis of the transgene products, we performed metabolic cell labeling experiments in combination with

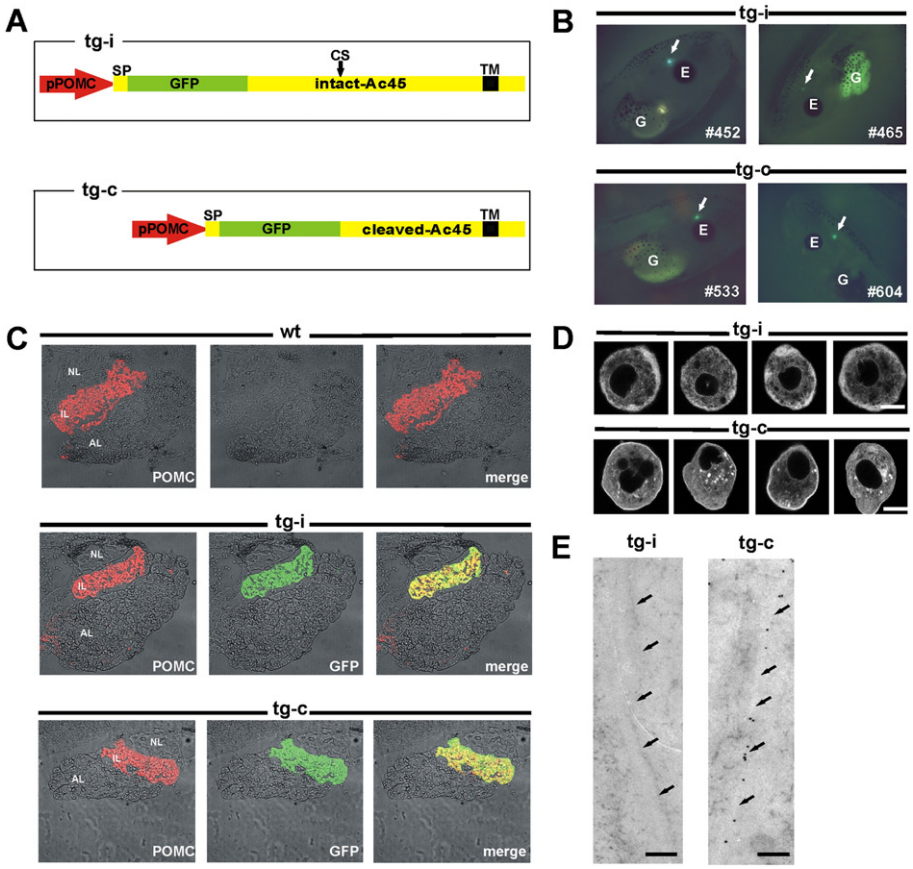

Fig. 1. Generation of transgenic *Xenopus laevis* with expression of GFP/intact-Ac45 or GFP/cleaved-Ac45 specifically in the intermediate pituitary melanotrope cells. (A) Schematic representation of the linear injection fragments used to generate transgenic *Xenopus*: pPOMC(A)$^{2+}$-SP-GFP/intact-Ac45 (tg-i) and pPOMC(A)$^{2+}$-SP-GFP/cleaved-Ac45 (tg-c) with the POMC-gene A promoter fragment (pPOMC), the regions encoding the GFP/intact-Ac45 or GFP/cleaved-Ac45 fusion protein and the SV40 polyadenylation signal (SV40 pA). SP: signal peptide; CS: cleavage site; TM: transmembrane region. (B) Transgenic stage-45 *Xenopus* tadpoles from lines #452 and #465 expressing GFP/intact-Ac45 and lines #533 and #604 expressing GFP/cleaved-Ac45 specifically in the intermediate pituitary (white arrow). E: eye; G: gut. (C) Sagittal brain-pituitary cryosections of wild-type (wt), GFP/intact-Ac45-transgenic (tg-i) and GFP/cleaved-Ac45-transgenic (tg-c) *Xenopus*. Transgene expression (green) was detected by direct fluorescence microscopy and endogenous POMC expression (red) by immunostaining with an anti-POMC antibody. All images were merged with bright-field captures, allowing visualization of the morphology of the pituitaries. NL: neural lobe, IL: intermediate lobe, AL: anterior lobe. (D) Direct CLSM on live melanotrope cells isolated from intermediate lobes expressing GFP/intact-Ac45 (#452) or GFP/cleaved-Ac45 (#533). The intact-Ac45 transgene product was localized mainly to the ER, whereas the cleaved-Ac45 transgene product was localized mainly to the plasma membrane. Note that in the active melanotrope cells the ER is situated near the plasma membrane [43]. Bar equals 5 μm. (E) Immunogold labeling of ultra-thin sections of transgenic melanotrope cells with the anti-GFP antibody in combination with 10-nm protein-A gold showing the absence of GFP/intact-Ac45 (tg-i, #452) and the presence of GFP/cleaved-Ac45 (tg-c, #533) at the plasma membrane. Arrows indicate the plasma membrane of the cells. Bars equal 100 nm.

immunoprecipitations using the anti-GFP or the anti-Ac45-C antibody. Analysis of the NILs transgenic for GFP/intact-Ac45 revealed the biosynthesis of an ~90-kDa newly synthesized GFP/-intact Ac45 fusion protein, whereas labeling of the GFP/cleaved-Ac45 transgenic NILs showed an ~70 kDa newly synthesized GFP/cleaved-Ac45 product (Fig. 2B). These newly synthesized proteins were recognized by both antibodies and corresponded to the major steady-state transgene products (Fig. 2A). Following a 30-min pulse and 8-h chase period only a minor portion of the 90-kDa newly synthesized GFP/intact-Ac45 fusion protein was cleaved (data not shown), suggesting that the rate of endoproteolytic processing of the intact Ac45-transgene product was low. Although the presence of the low amount of cleaved-Ac45 transgene product may be due to an insufficient availability of the Ac45 endoprotease, the cleavage rate of endogenous Ac45 has been found to be remarkably low as well [17].

Together, the microscopy, Western blot and biosynthetic studies revealed that the GFP/intact-Ac45 fusion protein was inefficiently transported and poorly cleaved, whereas the GFP/cleaved-Ac45 transgene product was efficiently transported to the plasma membrane. For our functional studies, we decided to focus on the transgenic line expressing the GFP/cleaved-Ac45 transgene product (hereafter referred to as the Ac45-transgene product), because this product corresponds to the predominant form of endogenous Ac45 (cleaved Ac45) that is also transported to the late stages of the secretory pathway [10].

3.2. Excess Ac45 displaces endogenous Ac45 but does not affect the levels of POMC and V-ATPase subunits A and E

Western blot analysis using the anti-Ac45-C antibody revealed that in the transgenic melanotrope cells the amount of the Ac45-transgene product was ~10-fold higher than the endogenous Ac45 protein level in wild-type cells, whereas the transgenic cells were devoid of endogenous Ac45 (Fig. 3A). Using anti-V-ATPase V_1A and V_1E subunit antibodies, similar steady-state expression levels for these V-ATPase subunits were found in wild-type and the Ac45-transgenic cells (Fig. 3B). Antibodies raised against synthetic peptides corresponding to regions within *Xenopus* V-ATPase subunits V_0a and V_0d did not recognize the endogenous V-ATPase subunits. In the wild-type and transgenic cells, similar steady-state levels of the main melanotrope cargo protein POMC were detected (Fig. 3C). We conclude that in the transgenic melanotrope cells the exogenous Ac45 effectively displaced endogenous Ac45 but did not affect the expression level of the endogenous V-ATPase nor of POMC.

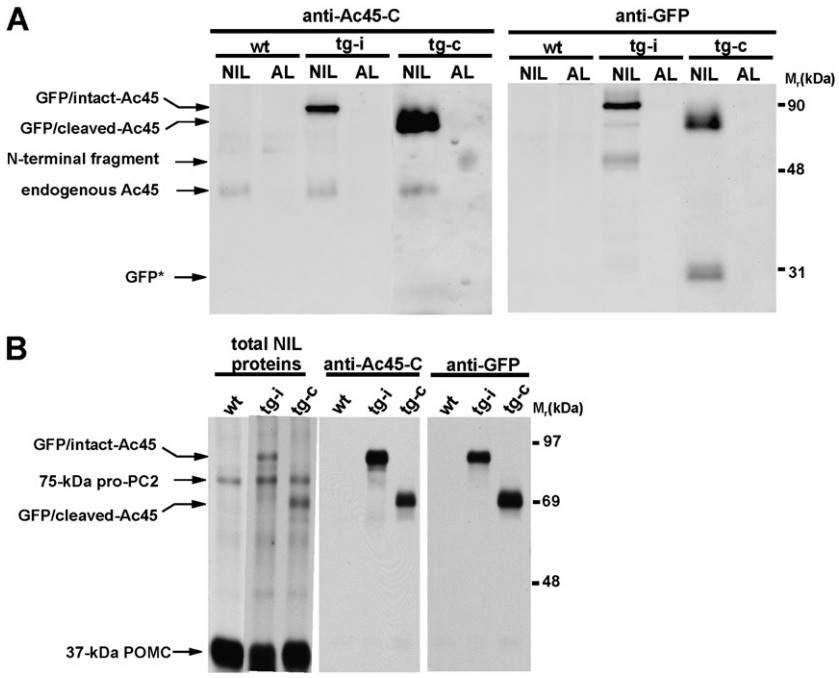

Fig. 2. Expression of the GFP/intact-Ac45 and GFP/cleaved-Ac45 transgene products in the *Xenopus* intermediate pituitary melanotrope cells. (A) Western blot analysis of GFP/intact-Ac45 (i) and GFP/cleaved-Ac45 (c) fusion protein expression in the neurointermediate lobe (NIL) and the anterior lobe (AL) of wild-type (wt) and transgenic (tg) *Xenopus* using an anti-Ac45-C or an anti-GFP antibody. The ~28 kDa protein detected by the anti-GFP, but not the anti-Ac45-C, antibody presumably represents the stable GFP moiety of trimmed fusion protein. (B) Analysis of newly synthesized proteins produced in NILs from wt and Ac45-transgenic *Xenopus*. NILs were pulse labeled for 2 h and 10% of the total NIL lysates was directly analyzed (lanes 1–3), whereas the remainder was immunoprecipitated using the anti-Ac45-C (lanes 4–6) or the anti-GFP (lanes 7–9) antibody and proteins were visualized by autoradiography.

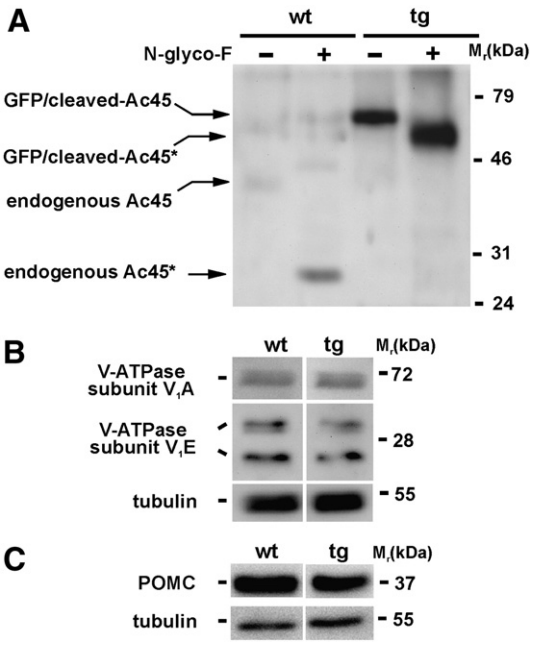

Fig. 3. Excess Ac45 displaces the endogenous Ac45 protein but does not affect the expression levels of the endogenous V-ATPase subunits V_1A and V_1E, and of POMC in the transgenic *Xenopus* melanotrope cells. (A) Western blot analysis of total proteins (10 μg) isolated from wild-type and Ac45-transgenic melanotrope cells using the anti-Ac45-C antibody. Since the Ac45 protein is more readily detected when deglycosylated, proteins were treated without (−) or with (+) *N*-glycosidase-F prior to Western blotting. Deglycosylated proteins are indicated with an asterisk. Note that the transgenic melanotrope cells are devoid of endogenous Ac45. (B) Western blot analysis of total proteins (20 μg) isolated from wild-type and Ac45-transgenic melanotrope cells using antibodies directed against the V-ATPase subunit V_1A, the V-ATPase subunit V_1E and tubulin. The anti-V-ATPase E antibody recognizes two forms of the V-ATPase subunit E [31]. (C) Western blot analysis of the protein equivalent of 0.5 wild-type and 0.5 Ac45-transgenic NIL using an anti-POMC and an anti-tubulin antibody.

3.3. Excess Ac45 affects the subcellular localization of the endogenous V-ATPase

We next wondered about the subcellular localization of the Ac45-transgene product and of the endogenous V-ATPase. Direct CLSM on cryosections of the Ac45-transgenic NIL showed the presence of the transgene product at the plasma membrane (Fig. 4E and K), in line with our observation in cultured transgenic melanotrope cells (Fig. 1D), whereas no fluorescence was observed in the wild-type melanotrope cells (Fig. 4B and H). To localize the endogenous V-ATPase, cryosections of wild-type and Ac45-transgenic NILs were immuno-stained with the anti-V-ATPase subunit V_1A antibody. In the wild-type cells, the V-ATPase subunit V_1A was localized to cytoplasmic structures and not at the plasma membrane (Fig. 4A). In contrast, in the Ac45-transgenic cells virtually no cytoplasmic staining was observed and V_1A was detected at the plasma membrane (Fig. 4D), largely co-localizing with the Ac45-transgene product (Fig. 4F). Thus, the localization of the V-ATPase subunit V_1A was clearly different in the wild-type and Ac45-transgenic cells. The localization of the main melanotrope cargo protein POMC was comparable in the wild-type and transgenic cells (Fig. 4G–L).

We then studied the localization of the Ac45-transgene product and the endogenous V-ATPase by immuno-EM. Using an anti-GFP antibody, the Ac45-transgene product was found to be localized to Golgi structures (Fig. 5B), secretory granules (Fig. 5C) and, in line with our confocal fluorescence microscopy data (Figs. 1D and 4E, K), predominantly at the plasma membrane and preferentially in microvilli (Fig. 5A) that were induced in the transgenic cells (see below). Application of the anti-V-ATPase subunit V_1A, V_1E, V_0a and V_0d antibodies revealed that in wild-type cells the V-ATPase subunits were mainly localized in the cytoplasm and partially associated with vesicular structures, whereas virtually no label was found at the plasma membrane (Fig. 5D–G). In contrast, in the Ac45-transgenic melanotrope cells most of the label was observed in the microvillar structures at the plasma membrane and thus the

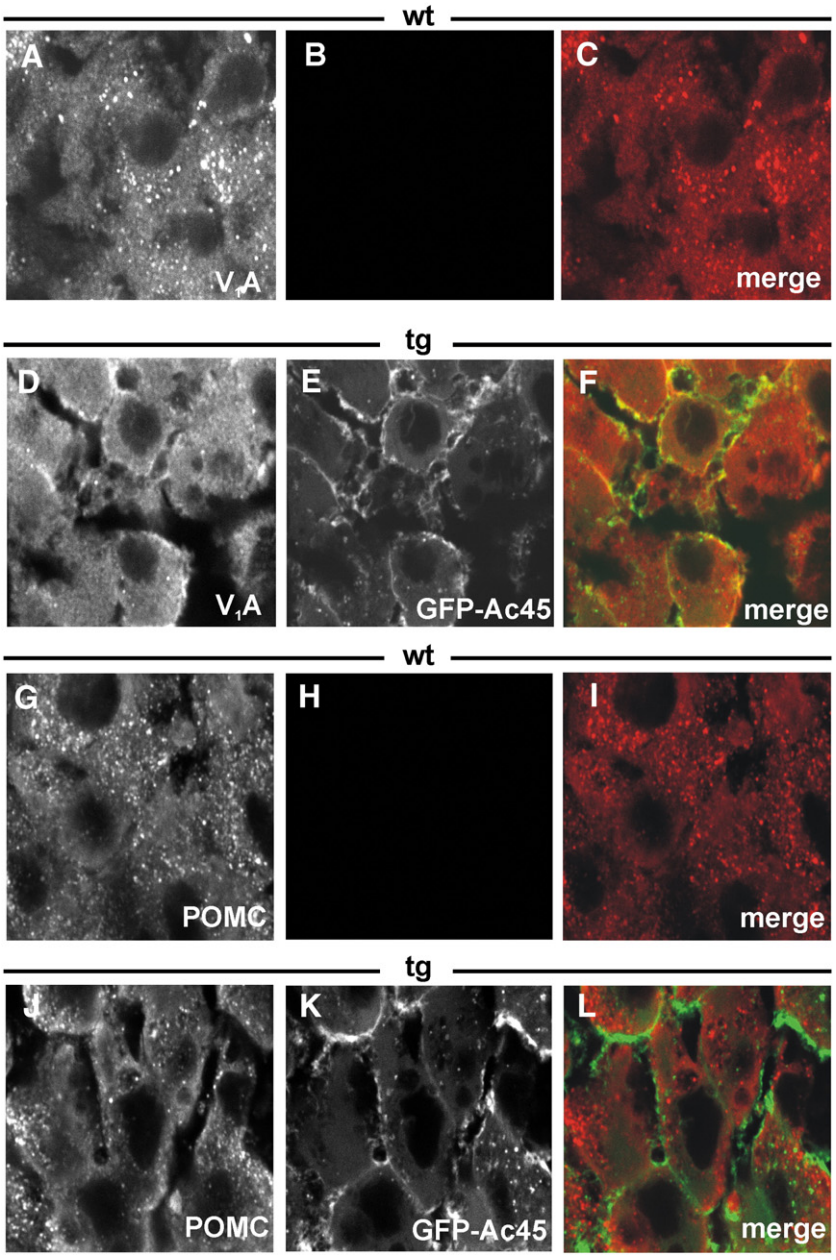

Fig. 4. Excess Ac45 affects the localization of the endogenous V-ATPase but does not affect POMC localization. Immunohistochemistry on sagittal brain-pituitary cryosections of wild-type (wt) *Xenopus* using anti-V-ATPase V_1A subunit antibodies revealed a punctuate cytoplasmic staining with no signal at the plasma membrane of the melanotrope cells (A), whereas in the Ac45-transgenic (tg) cells the localization of V-ATPase V_1A was predominantly at the plasma membrane (D), co-localizing with the Ac45-transgene product (F). Sagittal brain-pituitary cryosections of wt and tg *Xenopus* showed direct GFP fluorescence solely in the Ac45-transgenic cells and localized at the plasma membrane of the melanotrope cells (compare B, H with E, K). Immunohistochemistry with anti-POMC antibodies revealed similar granular POMC localization in both wt and tg cells (compare G and J) and no co-localization of POMC with the Ac45-transgene product was found (L).

endogenous V-ATPase subunits V_1A, V_1E, V_0a and V_0d were colocalized with the Ac45-transgene product at the surface of the transgenic cells (Fig. 5H–K).

From our immunofluorescence and immuno-EM data, we conclude that excess Ac45 shifted the majority of the endogenous V-ATPase towards the plasma membrane.

3.4. Excess Ac45 increases the number of dense-core secretory granules and affects plasma membrane morphology

We then performed TEM to study any morphological changes in the Ac45-transgenic melanotrope cells. Whereas the ultrastructure of a number of secretory pathway compartments, such as ER, Golgi and the immature dense-core secretory granules, was not affected in the transgenic cells (Fig. 6C, E), the number of immature dense-core granules per cell plane was significantly increased compared to that in wild-type cells (wt: 27.9±3.4/100 μm^2 cytoplasmic area, n=10, tg: 60.4±7.7/100 μm^2 cytoplasmic area, n=10, p<0.01). Immuno-EM using an anti-POMC antibody [30], revealed that in the Ac45-transgenic cells all immature secretory granules contained the prohormone (Fig. 6G). Furthermore, the Ac45-transgenic intermediate pituitaries were characterized by intercellular spaces that were not observed in the wild-type pituitaries (Fig. 6A, B). Moreover, in contrast to wild-type cells, the transgenic cells contained elaborate microvillar extensions of the plasma membrane that reached into the intercellular spaces (Fig. 6D, F). Together, our EM study showed that the

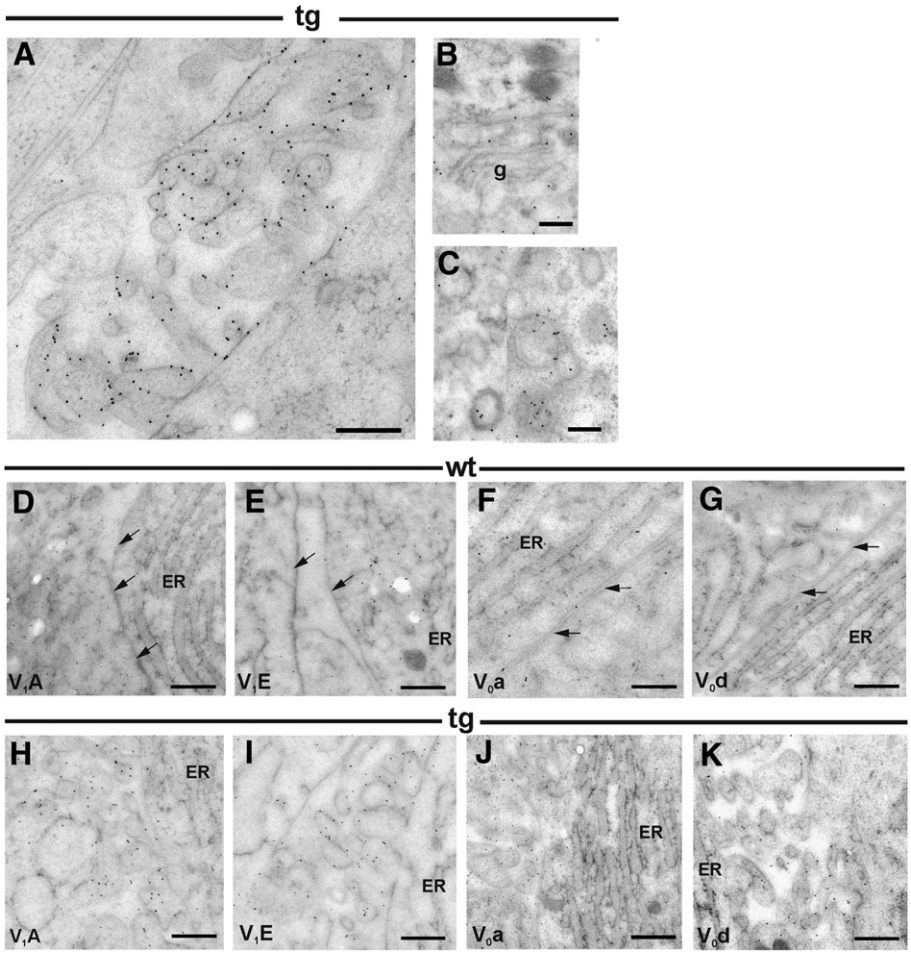

Fig. 5. Excess Ac45 shifts the localization of the endogenous V-ATPase to microvillar plasma membrane structures in the transgenic *Xenopus* melanotrope cells. (A–C) Immunogold labeling of ultra-thin sections of Ac45-transgenic (tg) melanotrope cells with the anti-GFP antibody in combination with 10-nm protein-A gold. Immunoreactivity was found in the microvillar extensions of the plasma membrane (A), the Golgi (B) and secretory granules (C). (D–K) Immunogold labeling of ultra-thin sections of wild-type (wt) and tg melanotrope cells using anti-V-ATPase subunit V_1A, V_1E, V_0a and V_0d antibodies in combination with 10-nm protein-A gold. In wt cells, the label was mainly found in the ER and the cytoplasm (D–G), whereas in the tg cells the antibodies reacted with the microvillar extensions of the plasma membrane (H–K). Arrows indicate the plasma membrane of the wt cells. Bars equal 100 nm.

ultrastructure of the Ac45-transgenic melanotrope cells was characterized by an increased number of immature, POMC-containing dense-core secretory granules and protrusions of the plasma membrane.

3.5. Excess Ac45 increases the secretion efficiency of the melanotrope cells

Since, as for other regulated secretory cells, in melanotrope cells the Ca^{2+}-influx is directly coupled to the efficiency of exocytosis [33,35], we decided to study the direct relationship between Ca^{2+}-influx and peptide secretion efficiency in the Ac45-transgenic cells. For this purpose, we determined the change in membrane capacitance (DCm) as a result of Ca^{2+}-charge (Q_{Ca}) upon induced membrane depolarizations in the whole-cell voltage-clamp patch-clamp mode. The wild-type (wt) and Ac45-transgenic (tg) melanotrope cells displayed comparable initial membrane capacitances (wt: 12.5 ± 0.91 pF, n = 10 *vs* tg: 10.9 ± 0.75 pF, n = 13) and similar Ca^{2+}-charges during a 50-ms depolarization from a DC holding potential of −80 mV to 0 mV (wt: 8.4 ± 1.2 pC, n = 10 *vs* tg: 8.1 ± 1.1 C, n = 13). Following such a single depolarizing pulse, the membrane capacitances of the wild-type and Ac45-transgenic cells increased as a result of vesicle fusion with the plasma membrane (Fig. 7A). In order to normalize for cellular variability in Q_{Ca}, we calculated the secretion efficiency (DCm/Q_{Ca}) in which the increase in membrane capacitance is directly correlated with the induced Ca^{2+}-charges [33]. Remarkably, following the single-pulse protocol the wild-type cells displayed a DCm/Q_{Ca} of 3.4 ± 0.32 fF/pC (n = 10), whereas the Ac45-transgenic melanotrope cells showed a significantly (2-fold) higher secretion efficiency (6.8 ± 0.63 fF/pC, n = 13, p < 0.001, Fig. 7A). We next applied a double-pulse protocol in which two 50-ms depolarizations were applied with a 200-ms interval. In wild-type melanotrope cells, this double-pulse protocol resulted in a larger increase of the membrane capacitance when compared to that following a single pulse, which was mainly determined by the occurrence of a slow, ~1 s-long increase in membrane capacitance after the second pulse. In the Ac45-transgenic cells, the double-pulse-induced increase in membrane capacitance was greatly enhanced compared to that in the wild-type cells, again largely due to the slow increase after the second pulse (Fig. 7B). The calculated secretion efficiency of the wild-type cells was 4.4 ± 0.38 fF/pC (n = 10), whereas the Ac45-transgenic cells showed a 3.4-fold (p < 0.001) higher DCm/Q_{Ca} (14.9 ± 2.3 fF/pC, n = 13) (Fig. 7B). We then determined the constitutive, Ca^{2+}-influx-independent secretion by measuring changes in membrane capacitance during a 30-s period in which no membrane depolarization was given. The Ca^{2+}-independent increase in membrane capacitance was found to be similar in both cell lines: 83.3 ± 2.2 fF/min in wild-type cells and 83.1 ± 1.3 fF/min in Ac45-transgenic cells. Taken together, these results indicate that excess

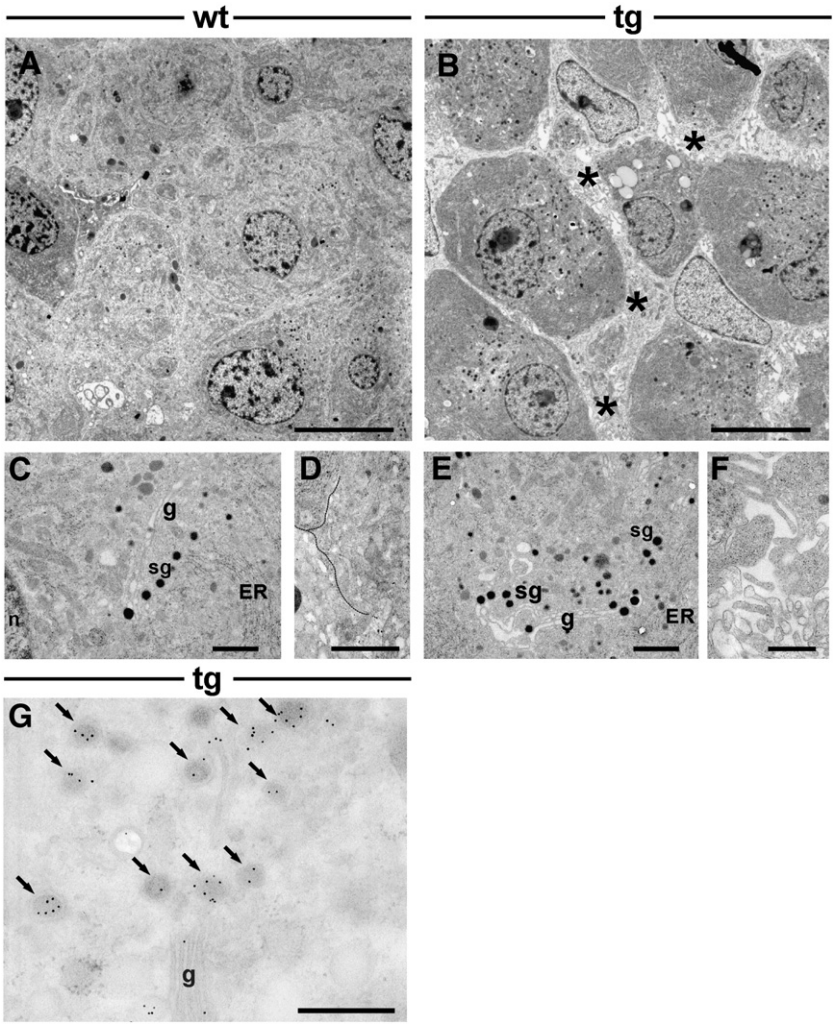

Fig. 6. The ultrastructure of the Ac45-transgenic *Xenopus* melanotrope cells is affected. Electron micrographs of intermediate pituitaries from wild-type (wt, A) and Ac45-transgenic (tg, B) animals. Intercellular spaces in the Ac45-transgenic intermediate pituitary are indicated with an asterisk. Bars equal 10 μm. (C–F) Electron micrographs of wt and tg melanotrope cells showing intracellular organelles such as nucleus (n), endoplasmic reticulum (ER), Golgi apparatus (g), secretory granules (sg) and plasma membrane (indicated with a dotted line). Microvillar extensions of the plasma membrane of tg melanotrope cells reaching into the intercellular spaces (F). Bars equal 1 μm. (G) Immunogold labeling of ultra-thin sections of the tg melanotrope cells with the anti-POMC antibody in combination with 10-nm protein-A gold. Immunoreactivity is restricted to the dense-core secretory granules (see arrows). Bar equals 200 nm.

Ac45 did not affect Ca^{2+}-independent exocytosis but rather increased the Ca^{2+}-dependent secretion efficiency of the transgenic *Xenopus* melanotrope cells.

4. Discussion

In this study, we explored the role of the intact and cleaved form of the type I transmembrane V-ATPase accessory subunit Ac45 in the strictly regulated *Xenopus* intermediate pituitary melanotrope cells. For this purpose, we employed stable *Xenopus laevis* transgenesis and used a *Xenopus* POMC-gene promoter fragment to drive Ac45-transgene expression specifically to the melanotrope cells. The rate of cleavage of the intact Ac45-transgene product was low, in line with the relatively low cleavage rate of endogenous Ac45 [17]. This intact Ac45-transgene product was localized mainly to the ER of the transgenic cells. In contrast, the cleaved Ac45-transgene product was predominantly situated at protrusions of the plasma membrane, indicating that it was efficiently transported through the secretory pathway. EM studies showed that intact-Ac45 expressing melanotrope cells (line #452) were indistinguishable from wild-type melanotrope cells and no protrusions were induced at the plasma membrane of these transgenic cells and no intercellular spaces were found between the transgenic cells (data not shown). Thus, cleavage of the Ac45 protein is apparently a prerequisite for its transport from ER to plasma membrane and the induction of the microvillar structures at the plasma membrane. Furthermore, the cleaved form represents the naturally occurring Ac45 associated with the V-ATPase in the late secretory pathway [10] We therefore focused on the analysis of the transgenic melanotrope cells expressing the cleaved Ac45-transgene product.

Our transgenic approach resulted in an ~10-fold steady-state excess of cleaved Ac45. The level of the newly synthesized endogenous Ac45 protein produced in the transgenic melanotrope cells was not affected (our unpublished observation), but the excess of Ac45 effectively displaced the endogenous Ac45 protein. The mechanism underlying the apparent removal of the endogenous Ac45 protein is at present unclear. Such a displacement event is however not unique since in transgenic *Xenopus* melanotrope cells expressing a p24δ_2-GFP or a p24α_3-GFP fusion protein all members of the endogenous type I transmembrane p24 protein family of putative ER-to-Golgi cargo receptors were effectively displaced by the transgene product as well [36,37]. Interestingly, whereas the transgenic manipulation did not affect the expression levels of POMC and the V-ATPase V_1 subunits A and E, the excess of Ac45 caused a shift in

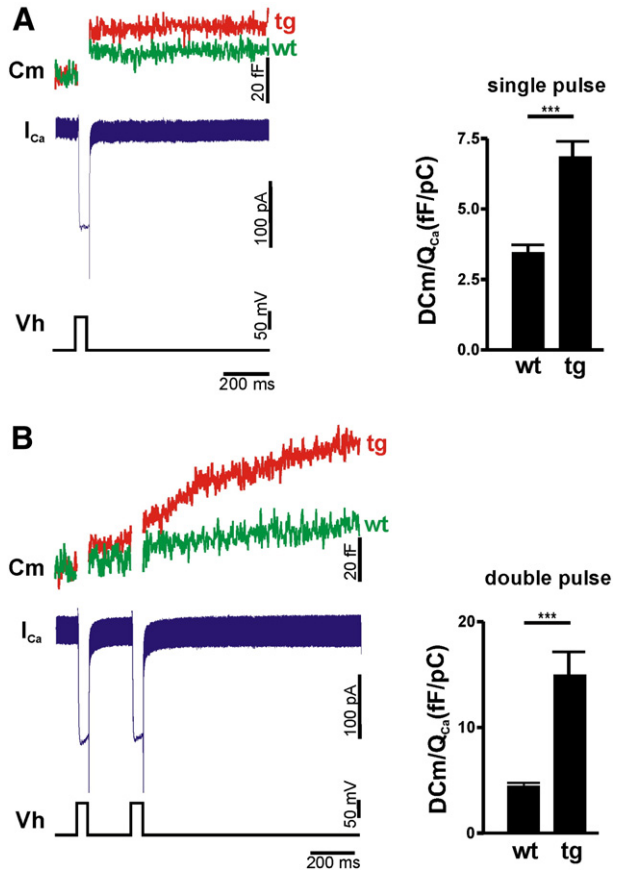

Fig. 7. The secretion efficiency is increased in the Ac45-transgenic *Xenopus* melanotrope cells. (A) Left: a single 50-ms depolarizing pulse (Vh) on wild-type (wt) and Ac45-transgenic (tg) melanotrope cells in the whole-cell voltage-clamp patch-clamp mode resulted in a Ca^{2+}-current (I_{Ca}). Prior to, and up to 1 s after the depolarizing pulse the membrane capacitance (Cm) was measured. Right: Quantification of the secretion efficiency (DCm/Q_{Ca}) of the wild-type ($n=10$) and the Ac45-transgenic ($n=13$) melanotrope cells following the single-pulse protocol. (B) Left: Two 50-ms depolarizing pulses were applied with a 200-ms interval, resulting in two similar Ca^{2+}-currents and a further raise in membrane capacitance. Right: quantification of the secretion efficiency (DCm/Q_{Ca}) of the wild-type ($n=10$) and the Ac45-transgenic ($n=13$) melanotrope cells following the double-pulse protocol. Shown are the means±SEM. Significant differences are indicated by *** ($p<0.001$).

the subcellular localization of the V-ATPase, namely preferentially to microvillar plasma membrane structures that were induced in the transgenic cells. The fact that the protrusions contained the majority of both the Ac45-transgene product and the V-ATPase V_1 and V_0 subunits indicated that the excess of Ac45 led to an efficient trafficking of the V-ATPase to the plasma membrane (with V_1 presumably piggy backing on the V_0 sector), apparently surpassing the capacity of V-ATPase endocytosis. It is at present unclear whether the excess of Ac45 also affected the endocytotic process.

We then examined the effect of excess Ac45 and of the resulting predominant localization of the V-ATPase system at the plasma membrane on the functioning of the transgenic *Xenopus* melanotrope cells. At the ultrastructural level we found a significantly higher number of immature secretory granules in the Ac45-transgenic melanotrope cells. Thus, excess Ac45 apparently provided an attractive microenvironment for the formation of immature secretory granules, a process that is known to be favored by a low pH in the TGN [38,39]. Furthermore, we performed patch-clamp experiments in the whole-cell voltage-clamp mode to study in an effective way the secretion efficiency of the transgenic melanotrope cells (the direct link between influx of $Ca^{2+}$and exocytosis). The observed significantly higher secretion efficiency in the transgenic cells was for a large part due to an increase in the slow secretory phase that lasted up to ~1 s after the depolarization. This phase is commonly associated with secretory granules that are either positioned more distant from the Ca^{2+}-channels, or are not docked and primed yet at the start of the Ca^{2+}-influx [40–42]. Interestingly, the effect of excess Ac45 was restricted to altering Ca^{2+}-dependent secretion because the drift in membrane capacitance, reflecting Ca^{2+}-independent exocytosis, was unaffected. We conclude that in the Ac45-transgenic cells only the regulated exocytotic machinery had been changed. Since we observed an increased number of secretory granules in the Ac45-transgenic cells, the augmented Ca^{2+}-dependent secretion is presumably the result of the presence of a larger pool of releasable granules. The notion of an increased rate of Ca^{2+}-dependent secretion is supported by our EM analyses that revealed, apart from the higher abundance of immature secretory granules, extensive protrusions of the plasma membrane, reflecting more efficient and accelerated exocytotic events in the Ac45-transgenic cells.

Collectively, our results indicated that Ac45 efficiently recruited the V-ATPase to the regulated secretory pathway, thereby acting as a modulator of the V-ATPase-mediated process of Ca^{2+}-dependent regulated peptide secretion. Intriguingly, such a neuroendocrine role for Ac45 is in line with the results of a very recent study showing that in the ruffled apical membranes of active osteoclasts Ac45 is also involved in a V-ATPase-mediated process, namely bone resorption [4]. In conclusion, our transgenic approach in a physiological context has provided for the first time functional data regarding the role of the V-ATPase accessory subunit Ac45 in neuroendocrine cells and the control of the V-ATPase in the regulated secretory pathway.

Acknowledgements

The authors thank Nick van Bakel, Marline van Hoek, Tim Arentsen, Tony Coenen and Peter Cruijsen for excellent technical assistance, Ron Engels for animal care, Dr. P. Jap (Radboud University Nijmegen, The Netherlands) for help with the interpretation of the EM data, Dr. B. Wieringa (Radboud University Nijmegen, The Netherlands) for providing the anti-GFP antibody and Dr. S. Tanaka (Shizuoka University, Japan) for providing the anti-V-ATPase subunit V_0a, V_0d, V_1A and V_1E antibodies.

References

[1] P. Paroutis, N. Touret, S. Grinstein, The pH of the secretory pathway: measurement, determinants, and regulation, Physiology (Bethesda) 19 (2004) 207–215.
[2] D.S. Adams, K.R. Robinson, T. Fukumoto, S. Yuan, R.C. Albertson, P. Yelick, L. Kuo, M. McSweeney, M. Levin, Early, H+-V-ATPase-dependent proton flux is necessary for consistent left-right patterning of non-mammalian vertebrates, Development 133 (2006) 1657–1671.
[3] T. Nishi, M. Forgac, The vacuolar (H+)-ATPases-nature's most versatile proton pumps, Nat. Rev. Mol. Cell. Biol. 3 (2002) 94–103.
[4] H. Feng, T. Cheng, N.J. Pavlos, K.H. Yip, A. Carrello, R. Seeber, K. Eidne, M.H. Zheng, J. Xu, Cytoplasmic terminus of a vacuolar type proton pump accessory subunit Ac45 is required for proper interaction with V0 domain subunits and efficient osteoclastic bone resorption, J. Biol. Chem. (2008).
[5] R.M. Weimer, E.M. Jorgensen, Controversies in synaptic vesicle exocytosis, J. Cell. Sci. 116 (2003) 3661–3666.
[6] N. Morel, Neurotransmitter release: the dark side of the vacuolar-H+ATPase, Biol. Cell. 95 (2003) 453–457.
[7] S. Liegeois, A. Benedetto, J.M. Garnier, Y. Schwab, M. Labouesse, The V0-ATPase mediates apical secretion of exosomes containing Hedgehog-related proteins in *Caenorhabditis elegans*, J. Cell. Biol. 173 (2006) 949–961.
[8] P.R. Hiesinger, A. Fayyazuddin, S.Q. Mehta, T. Rosenmund, K.L. Schulze, R.G. Zhai, P. Verstreken, Y. Cao, Y. Zhou, J. Kunz, H.J. Bellen, The v-ATPase V0 subunit a1 is required for a late step in synaptic vesicle exocytosis in *Drosophila*, Cell 121 (2005) 607–620.
[9] K.W. Beyenbach, H. Wieczorek, The V-type H+ATPase: molecular structure and function, physiological roles and regulation, J. Exp. Biol. 209 (2006) 577–589.
[10] F. Supek, L. Supekova, S. Mandiyan, Y.C. Pan, H. Nelson, N. Nelson, A novel accessory subunit for vacuolar H(+)-ATPase from chromaffin granules, J. Biol. Chem. 269 (1994) 24102–24106.
[11] V.T. Schoonderwoert, G.J. Martens, Proton pumping in the secretory pathway, J. Membr. Biol. 182 (2001) 159–169.
[12] F. Getlawi, A. Laslop, H. Schagger, J. Ludwig, J. Haywood, D. Apps, Chromaffin granule membrane glycoprotein IV is identical with Ac45, a membrane-integral subunit of the granule's H(+)-ATPase, Neurosci. Lett. 219 (1996) 13–16.

[13] J. Xu, T. Cheng, H.T. Feng, N.J. Pavlos, M.H. Zheng, Structure and function of V-ATPases in osteoclasts: potential therapeutic targets for the treatment of osteolysis, Histol. Histopathol. 22 (2007) 443–454.
[14] J. Ludwig, S. Kerscher, U. Brandt, K. Pfeiffer, F. Getlawi, D.K. Apps, H. Schagger, Identification and characterization of a novel 9.2-kDa membrane sector-associated protein of vacuolar proton-ATPase from chromaffin granules, J. Biol. Chem. 273 (1998) 10939–10947.
[15] J.C. Holthuis, E.J. Jansen, M.C. van Riel, G.J. Martens, Molecular probing of the secretory pathway in peptide hormone-producing cells, J. Cell. Sci. 108 (Pt 10) (1995) 3295–3305.
[16] J.C. Holthuis, E.J. Jansen, V.T. Schoonderwoert, J.P. Burbach, G.J. Martens, Biosynthesis of the vacuolar H+-ATPase accessory subunit Ac45 in *Xenopus* pituitary, Eur. J. Biochem. 262 (1999) 484–491.
[17] V.T. Schoonderwoert, E.J. Jansen, G.J. Martens, The fate of newly synthesized V-ATPase accessory subunit Ac45 in the secretory pathway, Eur. J. Biochem. 269 (2002) 1844–1853.
[18] B.G. Jenks, H.J. Leenders, G.J.M. Martens, E.W. Roubos, Adaptation physiology: the functioning of pituitary melanotrope cells during background adaptation of the amphibian *Xenopus laevis*, Zool. Sci. 10 (1993) 1–11.
[19] E.W. Roubos, Background adaptation by *Xenopus laevis*: a model for studying neuronal information processing in the pituitary pars intermedia, Comp. Biochem. Physiol. A. Physiol. 118 (1997) 533–550.
[20] H.Y. Zhang, M. Langeslag, M. Voncken, E.W. Roubos, W.J. Scheenen, Melanotrope cells of *Xenopus laevis* express multiple types of high-voltage-activated Ca2+channels, J. Neuroendocrinol. 17 (2005) 1–9.
[21] M.J. van den Hurk, W.J. Scheenen, E.W. Roubos, B.G. Jenks, Calcium influx through voltage-operated calcium channels is required for proopiomelanocortin protein expression in *Xenopus* melanotropes, Ann. N. Y. Acad. Sci. 1040 (2005) 494–497.
[22] B.G. Jenks, E.W. Roubos, W.J. Scheenen, Ca2+oscillations in melanotropes of *Xenopus laevis*: their generation, propagation, and function, Gen. Comp. Endocrinol. 131 (2003) 209–219.
[23] V.T. Schoonderwoert, G.J. Martens, Targeted disruption of the mouse gene encoding the V-ATPase accessory subunit Ac45, Mol. Membr. Biol. 19 (2002) 67–71.
[24] K.L. Kroll, E. Amaya, Transgenic *Xenopus* embryos from sperm nuclear transplantations reveal FGF signaling requirements during gastrulation, Development 122 (1996) 3173–3183.
[25] D.B. Sparrow, B. Latinkic, T.J. Mohun, A simplified method of generating transgenic *Xenopus*, Nucleic. Acids. Res. 28 (2000) E12.
[26] E.J. Jansen, T.M. Holling, F. van Herp, G.J. Martens, Transgene-driven protein expression specific to the intermediate pituitary melanotrope cells of *Xenopus laevis*, FEBS. Lett. 516 (2002) 201–207.
[27] E.J. Jansen, J.C. Holthuis, C. McGrouther, J.P. Burbach, G.J. Martens, Intracellular trafficking of the vacuolar H+-ATPase accessory subunit Ac45, J. Cell. Sci. 111 (Pt 20) (1998) 2999–3006.
[28] R.W. Collin, G.J. Martens, The coding sequence of amyloid-beta precursor protein APP contains a neural-specific promoter element, Brain. Res. 1087 (2006) 41–51.
[29] E. Cuppen, M. Wijers, J. Schepens, J. Fransen, B. Wieringa, W. Hendriks, A FERM domain governs apical confinement of PTP-BL in epithelial cells, J. Cell. Sci. 112 (Pt 19) (1999) 3299–3308.
[30] C.A. Berghs, S. Tanaka, F.J. Van Strien, S. Kurabuchi, E.W. Roubos, The secretory granule and pro-opiomelanocortin processing in *Xenopus* melanotrope cells during background adaptation, J. Histochem. Cytochem. 45 (1997) 1673–1682.
[31] S. Yajima, M. Kubota, T. Nakakura, T. Hasegawa, N. Katagiri, H. Tomura, Y. Sasayama, M. Suzuki, S. Tanaka, Cloning and expression of vacuolar proton-pumping ATPase subunits in the follicular epithelium of the bullfrog endolymphatic sac, Zoolog. Sci. 24 (2007) 147–157.
[32] D.T. Chu, M.W. Klymkowsky, The appearance of acetylated alpha-tubulin during early development and cellular differentiation in *Xenopus*, Dev. Biol. 136 (1989) 104–117.
[33] W.J. Scheenen, M.M. Dernison, J.R. Lieste, B.G. Jenks, E.W. Roubos, Electrical membrane activity and intracellular calcium buffering control exocytosis efficiency in *Xenopus* melanotrope cells, Neuroendocrinology 77 (2003) 153–161.
[34] M. Lindau, E. Neher, Patch-clamp techniques for time-resolved capacitance measurements in single cells, Pflugers. Arch. 411 (1988) 137–146.
[35] A. Tse, A.K. Lee, Voltage-gated Ca2+channels and intracellular Ca2+release regulate exocytosis in identified rat corticotrophs, J. Physiol. 528 (Pt 1) (2000) 79–90.
[36] G. Bouw, R. Van Huizen, E.J. Jansen, G.J. Martens, A cell-specific transgenic approach in *Xenopus* reveals the importance of a functional p24 system for a secretory cell, Mol. Biol. Cell. 15 (2004) 1244–1253.
[37] J.R. Strating, G. Bouw, T.G. Hafmans, G.J. Martens, Disparate effects of p24alpha and p24delta on secretory protein transport and processing, PLoS. ONE. 2 (2007) e704.
[38] E. Chanat, W.B. Huttner, Milieu-induced, selective aggregation of regulated secretory proteins in the trans-Golgi network, J. Cell. Biol. 115 (1991) 1505–1519.
[39] L. Taupenot, K.L. Harper, D.T. O'Connor, Role of H+-ATPase-mediated acidification in sorting and release of the regulated secretory protein chromogranin A: evidence for a vesiculogenic function, J. Biol. Chem. 280 (2005) 3885–3897.
[40] S.S. Stojilkovic, Pituitary cell type-specific electrical activity, calcium signaling and secretion, Biol. Res. 39 (2006) 403–423.
[41] K.D. Gillis, R. Mossner, E. Neher, Protein kinase C enhances exocytosis from chromaffin cells by increasing the size of the readily releasable pool of secretory granules, Neuron 16 (1996) 1209–1220.
[42] K.L. Engisch, N.I. Chernevskaya, M.C. Nowycky, Short-term changes in the Ca2+-exocytosis relationship during repetitive pulse protocols in bovine adrenal chromaffin cells, J. Neurosci. 17 (1997) 9010–9025.
[43] F. Van Herp, T. Coenen, H.P. Geurts, G.J. Janssen, G.J. Martens, A fast method to study the secretory activity of neuroendocrine cells at the ultrastructural level, J. Microsc. 218 (2005) 79–83.